

## NOTES AND CORRESPONDENCE

**The Influence of Cloud Droplets on the Measurement of Ice Particle Concentrations with a Particle Measuring System's 2DC Optical Array Probe**

ROBERT M. RAUBER

*Electronic Techniques, Inc., Auburn, California*

MARK F. HEGGLI

*Bureau of Reclamation, Auburn, California*

24 February 1987 and 1 June 1987

## ABSTRACT

The Particle Measuring System's 2DC optical array probe has been used as a primary instrument to measure ice particle concentrations since its introduction in 1976. In certain mixed-phase clouds containing cloud droplets in size ranges 30–100  $\mu\text{m}$ , the 2DC has been found to respond to both liquid and ice particles. This is of real concern, since ice crystals occur naturally in tens per liter, while supercooled droplets in this size range can occur in tens to hundreds per liter. In this note, the effect of cloud droplets on the measurement of ice particle concentrations with the 2DC probe is discussed. An example is presented where supercooled droplets overwhelm the probe, making accurate measurements of ice particle concentrations difficult to obtain.

**1. Introduction**

The Particle Measuring System's (PMS) two-dimensional cloud (2DC) optical array probe (OAP) has been the primary instrument used by many research programs to measure ice particle concentrations in clouds. Unambiguous measurements of ice particle concentrations with the probe depend on the ability of the user or instrument to discriminate water and ice particles. In the past, two methods of phase discrimination have been attempted, the first using polarization techniques (Knollenberg, 1981) and the second by applying sphericity tests to the images (Cooper, 1978; Heymsfield and Parrish, 1979).

Tests of the polarization system by PMS, discussed briefly by Knollenberg (1981), showed that 20%–30% of all crystals observed by the 2DC produce detectable polarization signals, and that the polarization signal is dependent on crystal orientation and habit. Cooper et al. (1982a) and Hobbs (1983) presented additional observational evidence that the detection efficiency for ice particles was 20%–30%. However, Cooper et al. (1982b) and Hobbs (1983) also found that 10%–15% of water droplets produced detectable changes in the polarization state of the 2DC. Cooper et al. noted that the signal from droplets was most likely to occur when droplets had sizes near the detection threshold (25–50  $\mu\text{m}$ ) of the instrument. Hobbs (1983) found that the

strength of the cross polarization signal was typically larger for ice particles. He used this observation and other 2DC data to develop an algorithm to estimate ice particle concentrations in mixed phase clouds. Hobbs' study suggests that the polarization signal may be used in some cases to aid in particle phase discrimination. However, more research is required to assess the ability of the instrument to determine particle phase reliably in a variety of mixed phase clouds.

The sphericity of images has been used in some applications to determine particle phase in mixed phase clouds (e.g., Sand et al., 1984). Sphericity tests of individual images can be used to discriminate phase provided that the cloud particles are of sizes of at least 150–200  $\mu\text{m}$ . Smaller size particles generally produce images too small to have a clear spherical shape. Such small images may be small ice particles, but can also be large cloud droplets.

In many cold ( $<0^{\circ}\text{C}$ ) cloud physics applications, specific image rejection criteria are applied to 2DC data (see Table 1) to eliminate images which may not be true cloud particles (e.g., Cooper, 1978; Gordon and Marwitz, 1986). In some cases, rejection criteria are not applied and the total particle count (referred to by PMS as the shadow—or concentration) is used to determine cloud particle concentrations (e.g., Heggli et al., 1983). With either method, small ( $<200 \mu\text{m}$ ) particles were normally retained in the accepted particle concentration measurement. Because particle size spectra are typically exponential, the smaller particles normally make a large contribution to the total measured particle concentration. These small particles are the subject of this note.

*Corresponding author address:* Dr. Robert Rauber, Dept. of Atmospheric Science, University of Illinois, 1101 W. Springfield Ave., Urbana, IL 61801.

TABLE 1. 2DC and 2DP image rejection criteria employed in postanalysis (from Gordon and Marwitz, 1986).

1. Streakers (usually, water shedding across the upstream edge of the probe and across the aperture) are rejected if they are six times as long (longitudinal dimension) as they are wide (lateral dimension). Images are also rejected as streakers (i) if they are three times as long as wide, (ii) if they are less than 150  $\mu\text{m}$  wide, and (iii) if they do not overlay the edge of the scan region (Cooper, 1978).
2. Cases in which the probe recording circuitry are triggered but no elements are recorded as shadowed (so-called "zero area" images) are rejected. These often correspond to true objects near the minimum size detectable by the probe (Cooper, 1978).
3. Images resulting from particles splashing off the edges of the aperture are eliminated by calculating the average distance between particles based on concentration and rejecting those particles that pass through the beam at times less than the time corresponding to the average distance.
4. Images having more than two gaps are rejected.

While conducting studies of cloud systems over the mountains of California during the Sierra Cooperative Pilot Project (Reynolds and Dennis, 1986), it has become evident that many cloud systems contain cloud droplets within the approximate size range 30–100  $\mu\text{m}$ . These droplets generally occur in low concentrations (0.1–0.5  $\text{cm}^{-3}$ ) and sometimes occur in regions of low liquid water content ( $<0.1 \text{ g m}^{-3}$ ). The source of these droplets is not always clear, but their effect on the measurement of ice particle concentrations with the 2DC is significant. In this note, we document the nature of the 2DC response to these large cloud droplets in two regions of cloud, the first composed almost entirely of droplets and the second, a mixed phase region which also contained large ice particles. We point out potential misinterpretations of cloud processes that can result if the contribution to the 2DC particle concentration by large cloud droplets is attributed instead to ice particles.

## 2. Instrumentation

Aircraft data were collected by the University of Wyoming Beechcraft Super King Air. The King Air is equipped with a full complement of cloud physics probes. Those discussed here include a Forward Scattering Spectrometer Probe (FSSP), operated in the 3–45  $\mu\text{m}$  range, an OAP 2DC operated in the 25–800  $\mu\text{m}$  range with 25  $\mu\text{m}$  resolution, and an OAP 2DP operated in the range 200–6400  $\mu\text{m}$  with 200  $\mu\text{m}$  intervals. Image rejection techniques used for the 2DC and 2DP data are summarized in Table 1. Liquid water probes include a Johnson Williams (JW) device, a Commonwealth Scientific and Industrial Organization (CSIRO) probe, the FSSP, and a Rosemount icing rate meter (RIM). Calibrations of the JW and FSSP probes used on the King Air are discussed by Strapp and Schemenauer (1982) and Cerni (1983) and are summarized by Sand et al. (1984). The response of CSIRO probes has been studied by King et al. (1985). Data from a 5-cm wavelength radar are also used. The radar is described by Huggins and Rodi (1985).

## 3. 12 February 1986 cloud system

The cloud system discussed here occurred on 12 February 1986, was orographic, had a 4 km depth

(cloud top temperature  $\geq -15^\circ\text{C}$ ), and extended upwind of the Sierra Crest about 130 km. Figure 1a shows a vertical profile of this cloud system, regions of de-

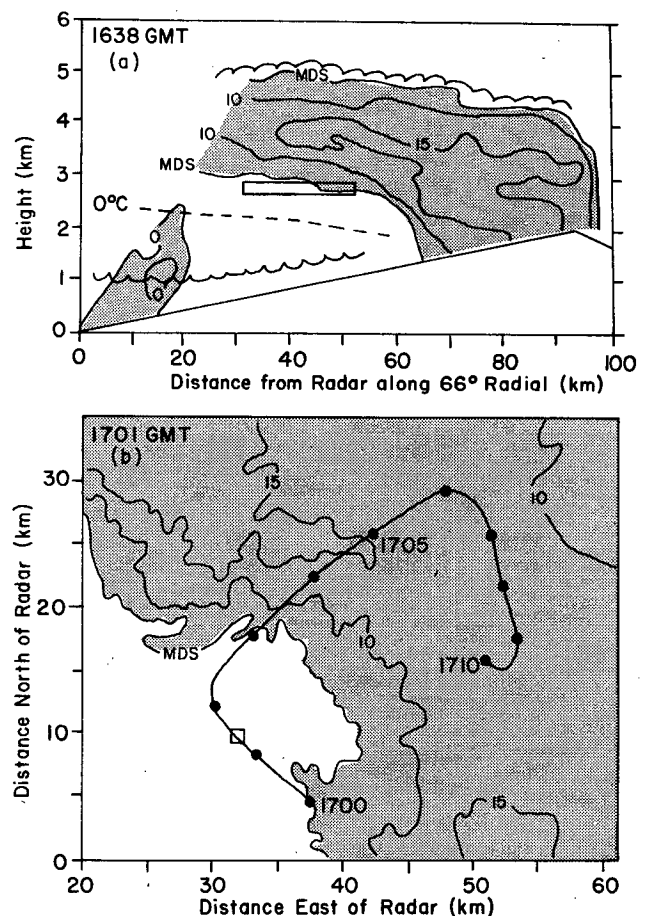


FIG. 1. (a) Vertical cross section of 12 February 1986 cloud system at 1638 UTC taken along 66° radial from the radar showing the radar reflectivity (dBZ), the approximate cloud boundaries based on aircraft measurements, the 0°C isotherm and the local topography. The box denotes the location of the flight discussed in the text. (b) Segment of planned position indicator (PPI) scan at 3.5° elevation showing radar reflectivity (dBZ) and the location of the flight track. The box along the flight track indicates the intersection point of the PPI plane with the aircraft. Times are UTC. Shaded regions on both figures denote where radar reflectivity exceeded the minimum detectable echo (3.9 dBZ at 50 km, 7.4 dBZ at 75 km).

tectable radar echo (shaded), the approximate cloud boundaries and the local topography. The segment of the flight of interest here occurred within the small box near the center of the figure. This segment was flown between 1700 and 1710 UTC at temperatures ranging from  $-3.5^{\circ}$  to  $-4.0^{\circ}\text{C}$ . Figure 1b shows a region of a planned position indicator (PPI) plot of radar reflectivity taken from a  $3.5^{\circ}$  scan at 1701 UTC. Reflectivities above minimum detectable echo are shaded. During the flight, the aircraft initially flew below the region of detectable echo. In this region, the aircraft encountered small ( $<100\ \mu\text{m}$ ) particles. As the aircraft turned northeast, it entered the region of descending echo evident on Fig. 1a. Within this region, a wide spectrum of particle sizes were observed. The remainder of this note will consider the response of the aircraft probes within these regions.

#### 4. Response of cloud probes

Figure 2 shows data for ten measurements obtained from six independent probes. These include the 2DC and 2DP total particle concentration (no image rejection), the 2DC and 2DP accepted particle concentration, the FSSP total particle concentration, the FSSP particle concentration in the three largest size ranges ( $36\text{--}45\ \mu\text{m}$ ), and liquid water content from the FSSP, CSIRO, JW, and RIM probes. Melt cycles of the RIM are indicated by the vertical line. The data spans a 10-minute period from 1700 to 1710 UTC. During this time period the aircraft flew from the nonechoing region of the cloud into the base of the descending cloud echo (see Fig. 1). 2DC and 2DP images from 170211–15 and 170621–27 UTC are shown in Fig. 3.

Consider first the data collected outside the echo region between 1701–1703. The presence of supercooled water was verified by all four probes within this region. FSSP droplet concentrations were measured at  $10\text{--}20\ \text{cm}^{-3}$ . Within the  $36\text{--}45\ \mu\text{m}$  size ranges of the FSSP, concentrations ranged from  $1.5\text{--}3.0\ \text{cm}^{-3}$  ( $1500\text{--}3000\ \text{L}^{-1}$ ). The magnitude of the liquid water on the CSIRO, FSSP and JW varied, with the CSIRO highest and JW lowest. Such behavior would be expected in the presence of large cloud droplets, since the JW probe had a cutoff in response for droplets larger than  $40\ \mu\text{m}$  diameter, while laboratory and field tests have indicated that the CSIRO probe has a partial response to drizzle and precipitation drops (King et al., 1985). Consider now the behavior of the OAPs. The 2DC total particle concentrations ranged from  $25\text{--}250\ \text{L}^{-1}$ . After applying image rejection criteria, the concentrations reduced to about half these values. Virtually all rejected images were “zero area” images. The 2DP, both corrected and uncorrected concentrations, were near zero throughout the period. Several peaks in the 2DC particle concentrations corresponded precisely with peaks in the CSIRO liquid water content. Zero area images and 1–2 diode occlusions were the most typical image on the

2DC (Fig. 3). Recent work of Baumgardner et al. (1986) indicates that the 2DC is probably insensitive to particles smaller than  $\sim 50\ \mu\text{m}$ . Based on the liquid water measurements, cloud droplets with sizes greater than this threshold were likely to exist in this cloud. The environment was highly conducive to ice particle growth by diffusion and riming yet no particles were detected by the 2DP. The absence of particles within the 2DP size range, the absence of a radar echo, the correspondence between peaks on the liquid water and OAP probes, the consistency in the liquid water measurements, and the large concentration of droplets within the larger FSSP size ranges together imply that the 2DC was responding to cloud droplets.

Consider now the data collected in the mixed phase region between 1705–1708 UTC. Trends in liquid water content were similar—the CSIRO liquid water content was largest in magnitude, followed by the FSSP and JW. Such a trend again indicates large drops were present. The FSSP droplet concentration remained in the  $10\text{--}20\ \text{cm}^{-3}$  range but the concentration of droplets in the largest size range peaked at  $6\text{--}9\ \text{cm}^{-3}$ . Within this region, ice particles were present (see Fig. 3), but the values of concentrations measured by the OAPs varied by as much as two and one-half orders of magnitude. For example, at the peak liquid water measurement by the CSIRO at 170630, the corrected 2DC measurement was  $200\ \text{L}^{-1}$  while the corrected 2DP was  $<1\ \text{L}^{-1}$ . Again, the majority of the images were “zero area” or 1–2 diode occlusions on the 2DC. Liquid water peaks corresponded extremely well with peaks in particle concentrations measured within the FSSP largest size range, as well as the 2DC. For the same reasons as outlined above, the OAP 2DC probe appeared to be responding to cloud droplets larger than  $\sim 50\ \mu\text{m}$ .

#### 5. Discussion

The measurement of ice particle concentrations is important to most aspects of cloud physics research. Since the introduction of the 2DC, the probe has been the primary instrument to measure ice particle concentrations. In this note, we have shown that particle concentrations measured by the 2DC probe can be influenced to a large degree by the presence of large cloud droplets. We have demonstrated that cloud droplets can make a significant contribution to the measured 2DC particle concentration even in regions of very low liquid water content.

Conditions shown in this cloud system are not unusual over the Sierra Nevada. Since the analysis of this case was completed, regions of many other cloud systems have been identified where droplets may be contributing to the 2DC concentration measurement. Occasionally, liquid water content measured in these regions was as low as  $0.05\text{--}0.10\ \text{g m}^{-3}$ . In most cases,

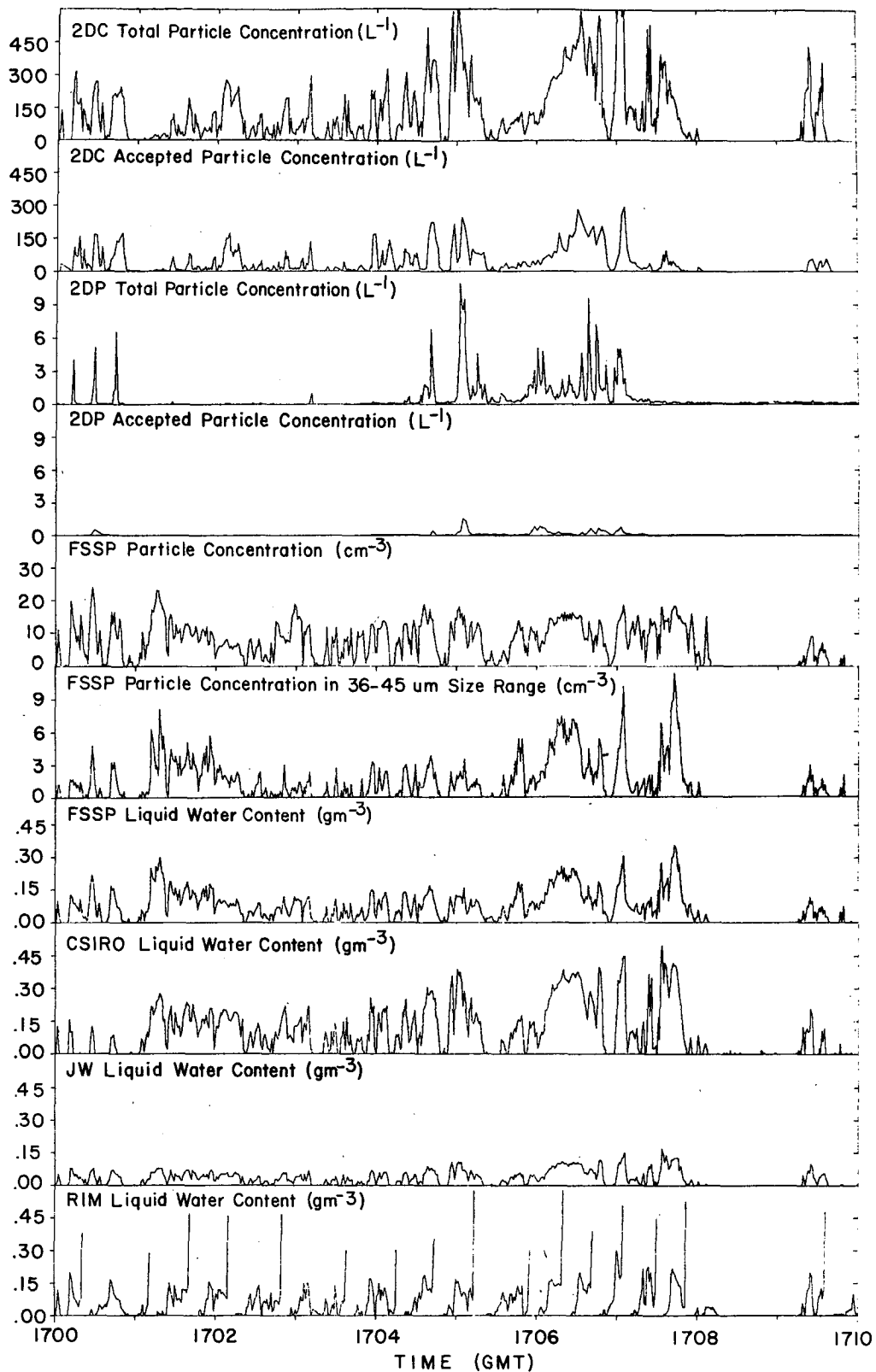


FIG. 2. King Air measurements between 1700 and 1710 UTC. The data are described in the text.

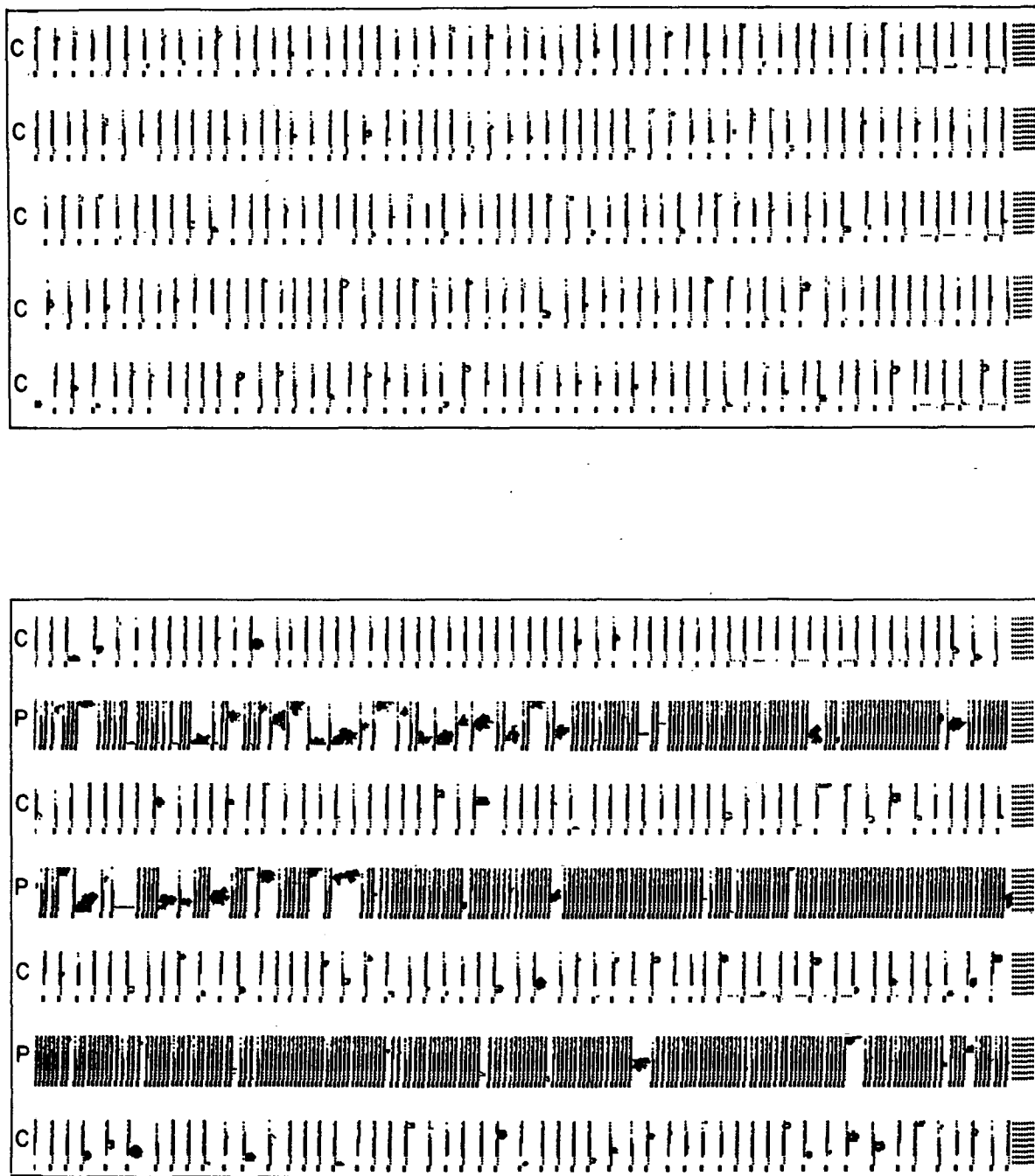


FIG. 3. (Top) 2DC images from 1702:11-1702:15 UTC. (Bottom) 2DC and 2DP images from 1706:21-1706:27 UTC. The scales of the vertical bars on the 2DC and 2DP images are, respectively, 800 and 6500  $\mu\text{m}$ .

the phase of the particles could only be inferred by the response of independent instrumentation.

Although cloud systems over different geographic regions will have different physical characteristics, the low concentrations of large cloud droplets required to affect substantially the 2DC is cause for concern. For example, larger droplets in concentrations of only  $0.01 \text{ cm}^{-3}$  have the potential to produce a  $10 \text{ L}^{-1}$  change

in particle concentration measured by the 2DC. Based on these results, caution should be exercised when interpreting the characteristics of small images of the 2DC probe taken in mixed phase cloud systems, particularly since small particles often provide the greatest contribution to the total particle concentration. This is particularly important in regions of clouds where the Hallett-Mossop mechanism is suspected to operate

(e.g., Marwitz, 1987), since a major requirement for the Hallett–Mossop mechanism is the presence of large cloud droplets. Until well-tested methods of phase discrimination become available, 2DC concentrations should be carefully assessed to determine particle phase by considering the response of independent probes within the same cloud regions.

*Acknowledgments.* This work was supported by U.S. Bureau of Reclamation Contract 4-CR-81-03860. The authors would like to thank all of the participants in the SCPP program. Special thanks to the University of Wyoming for supplying the King Air data, and the staff of Electronic Techniques, Inc., particularly Mr. Arlen Huggins for assistance in the analysis, Mr. Arunas Kuciauskas who processed the radar data, and Ms. Carol Wilcox who drafted the figures and typed the manuscript.

#### REFERENCES

- Baumgardner, D., J. E. Dye and W. A. Cooper, 1986: The effects of measurement uncertainties on the analysis of cloud particle data. *Preprints, Joint Conf. on Cloud Physics and Radar Meteorology*, Snowmass, Amer. Meteor. Soc., pp. JP313–JP316.
- Cerni, T. A., 1983: Determination of the size and concentration of cloud drops with an FSSP. *J. Climate Appl. Meteor.*, **22**, 1346–1355.
- Cooper, W. A., 1978: Cloud physics investigations by the University of Wyoming in HIPLEX, 1977. Rep. AS119, Dept. of Atmospheric Science, University of Wyoming, 320 pp.
- , R. P. Lawson and T. A. Cerni, 1982a: Cloud physics investigations by the University of Wyoming in HIPLEX 1979. Dept. of Atmospheric Science, University of Wyoming, 301 pp.
- , T. A. Cerni and A. R. Rodi, 1982b: Cloud physics investigations, University of Wyoming, 1978. Rep. AS137, Dept. of Atmospheric Science, University of Wyoming, 298 pp.
- Gordon, G. L., and J. D. Marwitz, 1986: Hydrometer evolution in rainbands over the California valley. *J. Atmos. Sci.*, **43**, 1087–1100.
- Heggl, M. F., L. Vardiman, R. E. Stewart and A. Huggins, 1983: Supercooled liquid water and ice crystal distributions within Sierra Nevada winter storms. *J. Climate Appl. Meteor.*, **22**, 1875–1886.
- Heymsfield, A. J., and J. L. Parrish, 1979: Techniques employed in the processing of particle size spectra and state parameter data obtained with the T-28 aircraft platform. NCAR Tech. Note, NCAR/TN-137-1A, CSD.
- Hobbs, R. A., 1983: Field studies of secondary ice crystal production. Ph.D. dissertation, University of Wyoming, 320 pp.
- Huggins, A. W., and A. R. Rodi, 1985: Physical response of convective clouds over the Sierra Nevada to seeding with dry ice. *J. Climate Appl. Meteor.*, **24**, 1082–1098.
- King, W. D., J. E. Dye, J. W. Strapp, D. Baumgardner and D. Huffman, 1985: Icing wind tunnel tests on the CSIRO liquid water probe. *J. Atmos. Oceanic Technol.*, **2**, 340–352.
- Knollenberg, R. G., 1981: Techniques for probing cloud microstructure. *Clouds: Their Formation, Optical Properties and Effects*, P. V. Hobbs and A. Deepak, Eds., Academic Press, 15–91.
- Marwitz, J. D., 1987: Deep orographic storms over the Sierra Nevada. Part II: The precipitation processes. *J. Atmos. Sci.*, **44**, 174–185.
- Reynolds, D. W., and A. S. Dennis, 1986: A review of the Sierra Cooperative Pilot Project. *Bull. Amer. Meteor. Soc.*, **67**, 513–523.
- Sand, W. R., W. A. Cooper, M. K. Politovich and D. L. Veal, 1984: Icing conditions encountered by a research aircraft. *J. Climate Appl. Meteor.*, **23**, 1427–1440.
- Strapp, J. W., and R. S. Schemenauer, 1982: Calibrations of Johnson–Williams liquid water content meters in a high speed icing tunnel. *J. Appl. Meteor.*, **21**, 98–108.